

## The ABCG2 efflux transporter from rabbit placenta: cloning and functional characterization

Sandra Halwachs, Carsten Kneuer, Katrin Gohlsch, Marian Müller, Vera Ritz,  
Walther Honscha

### Angaben zur Veröffentlichung / Publication details:

Halwachs, Sandra, Carsten Kneuer, Katrin Gohlsch, Marian Müller, Vera Ritz, and Walther Honscha. 2016. "The ABCG2 efflux transporter from rabbit placenta: cloning and functional characterization." *Placenta* 38: 8-15.  
<https://doi.org/10.1016/j.placenta.2015.12.005>.



## The ABCG2 efflux transporter from rabbit placenta: Cloning and functional characterization



Sandra Halwachs<sup>a,\*</sup>, Carsten Kneuer<sup>b</sup>, Katrin Gohlsch<sup>b,1</sup>, Marian Müller<sup>a</sup>, Vera Ritz<sup>b</sup>, Walther Honscha<sup>a</sup>

<sup>a</sup> Institute of Pharmacology, Pharmacy and Toxicology, Faculty of Veterinary Medicine, Universität Leipzig, An den Tierkliniken 15, D-04103 Leipzig, Germany

<sup>b</sup> Federal Institute for Risk Assessment (BfR), Pesticide Safety, Max-Dohrn-Straße 8-10, D-10589 Berlin, Germany

### ARTICLE INFO

#### Article history:

Received 13 October 2015

Received in revised form

12 November 2015

Accepted 10 December 2015

#### Keywords:

ABCG2/BCRP efflux transporter

Placenta barrier

Rabbit

developmental toxicity testing

Active drug transport

MDCKII in vitro model

### ABSTRACT

In human placenta, the ATP-binding cassette efflux transporter ABCG2 is highly expressed in syncytiotrophoblast cells and mediates cellular excretion of various drugs and toxins. Hence, physiological ABCG2 activity substantially contributes to the fetoprotective placenta barrier function during gestation. Developmental toxicity studies are often performed in rabbit. However, despite its toxicological relevance, there is no data so far on functional ABCG2 expression in this species. Therefore, we cloned ABCG2 from placenta tissues of chinchilla rabbit. Sequencing showed 84–86% amino acid sequence identity to the orthologues from man, rat and mouse. We transduced the rabbit ABCG2 clone (rbABCG2) in MDCKII cells and stable rbABCG2 gene and protein expression was shown by RT-PCR and Western blot analysis. The rbABCG2 efflux activity was demonstrated with the Hoechst H33342 assay using the specific ABCG2 inhibitor Ko143. We further tested the effect of established human ABCG2 (hABCG2) drug substrates including the antibiotic danofloxacin or the histamine H<sub>2</sub>-receptor antagonist cimetidine on H33342 accumulation in MDCKII-rbABCG2 or -hABCG2 cells. Human therapeutic plasma concentrations of all tested drugs caused a comparable competitive inhibition of H33342 excretion in both ABCG2 clones. Altogether, we first showed functional expression of the ABCG2 efflux transporter in rabbit placenta. Moreover, our data suggest a similar drug substrate spectrum of the rabbit and the human ABCG2 efflux transporter.

© 2015 The Authors. Published by Elsevier Ltd. This is an open access article under the CC BY-NC-ND license (<http://creativecommons.org/licenses/by-nc-nd/4.0/>).

**Abbreviations:** ABCG2, ATP-binding cassette sub-family G member 2; cDNA, complementary DNA; DMEM, Dulbecco's modified Eagle's medium; dNTP, 2'-deoxynucleoside-5'-triphosphate; Ko143, 3-((3S,6S,12aS)-6-isobutyl-9-methoxy-1,4-dioxo-1,2,3,4,6,7,12,12a-octa-hydropyrazino [1,2:1,6]pyrido [3,4-b]indol-3-yl)-propionic acid tert-butyl ester; MDCKII-WT cells, Madin–Darby canine kidney (MDCK) type II wild type cells; Mr, relative molecular mass; nt, nucleotides; ORF, open reading frame; RACE, rapid amplification of cDNA ends; rbABCG2, rabbit ABCG2; RFU, relative fluorescence unit; UTR, untranslated region.

\* Corresponding author. Institute of Pharmacology, Pharmacy and Toxicology, Faculty of Veterinary Medicine, Universität Leipzig, Leipzig, Germany.

**E-mail addresses:** [halwachs@vetmed.uni-leipzig.de](mailto:halwachs@vetmed.uni-leipzig.de) (S. Halwachs), [Carsten.Kneuer@bfr.bund.de](mailto:Carsten.Kneuer@bfr.bund.de) (C. Kneuer), [gohlsch.katrin@gmx.de](mailto:gohlsch.katrin@gmx.de) (K. Gohlsch), [loki.mm21@web.de](mailto:loki.mm21@web.de) (M. Müller), [Vera.Ritz@bfr.bund.de](mailto:Vera.Ritz@bfr.bund.de) (V. Ritz), [honscha@vetmed.uni-leipzig.de](mailto:honscha@vetmed.uni-leipzig.de) (W. Honscha).

<sup>1</sup> Present address: Walther-Straub-Institute for Pharmacology and Toxicology, Ludwig-Maximilians-Universität München, Goethestraße 33, 80336 München, Germany.

<http://dx.doi.org/10.1016/j.placenta.2015.12.005>

0143-4004/© 2015 The Authors. Published by Elsevier Ltd. This is an open access article under the CC BY-NC-ND license (<http://creativecommons.org/licenses/by-nc-nd/4.0/>).

### 1. Introduction

The placenta serves as a protective barrier by limiting the transfer of potential toxic xenobiotics from maternal circulation to the developing fetus. It has recently been suggested that expression of ATP-binding cassette (ABC) efflux transporters in placenta including ABCG2 makes an important contribution to this protective mechanism [1]. The 72 kDa half-transporter ABCG2 also referred to as breast cancer resistance protein (BCRP) shows high level expression in placenta and was therefore initially named ABCP (ABC transporter in placenta) [2]. In the human and murine placenta barrier, the ABCG2 transport protein is localized at the apical membrane of syncytiotrophoblast cells, i.e. on the maternal side [1,3]. The placental ABCG2 mediates cellular excretion of various drugs and toxins like the antidiabetic drug glyburide, the antibiotic nitrofurantoin or the dietary pro-carcinogen 2-Amino-1-methyl-6-phenyl-imidazo[4,5-b]pyridine (PhIP) [4–6]. Hence, the physiological ABCG2 efflux activity limits fetal exposure to

potential harmful xenobiotics.

The preferred rodent and non-rodent species for testing of prenatal developmental toxicity are rat and rabbit, respectively [7]. Compared with rodents which develop a hemotrichorial placenta, the hemodichorial structure of the rabbit placenta is closer to the hemomonochorial morphology of human placenta in the last trimester [8]. Moreover, the placental function of rabbit placenta is similar to human [8]. This, along with practical consideration, e.g. about fetus size, made this species a valuable model for human health hazard assessment. Accordingly, studies on developmental toxicity in rabbits are preferred over rat studies for biocides (Regulation (EU) No. 528/2013) or included in legislative data requirements for pesticides (Regulation (EU) No. 283/2013) and other chemicals. Consequently, 2560 rabbits are used for developmental toxicity testing in safety evaluations during 2011 in the EU alone [9]. In spite of the significant fetoprotective function of placental ABCG2 and the regulatory importance of the rabbit in reproductive studies, no detailed information is as yet available on the active transport of xenobiotics across the rabbit placenta and the contribution of the ABCG2 efflux transporter. At the time of the initiation of our study, there was only a predicted rabbit ABCG2 mRNA sequence available (NCBI Nucleotide Database, Accession No. XM\_002716965.1, accessed 09/30/2011). Compared to the human and rat or mice orthologues, the corresponding polypeptide sequence showed a central deletion. This deletion would very likely result in a non-functional translation product. Additionally, there was no clear information about functional activity of the ABCG2 transporter in rabbit [10,11]. In this study, we therefore cloned and sequenced ABCG2 cDNA from rabbit placenta tissues (rbABCG2). Moreover, we generated MDCKII cells stably expressing rbABCG2. Using this cell line, we investigated the functional rbABCG2 activity and compared its substrate specificity with that of the human ABCG2 transporter.

## 2. Materials and methods

### 2.1. Reagents

Hoechst H33342 was from AppliChem (Darmstadt, Germany), Ko143, nitrofurantoin (NF), methotrexate (amethopterin, MTX) from Sigma–Aldrich (Deisenhofen, Germany), cimetidine and PhIP from Santa Cruz Biotechnology (Heidelberg, Germany) and danofloxacin mesylate (DFM) from Dr. Ehrenstorfer Inc. (Augsburg, Germany). All chemicals were purchased at analytical grade. Oligonucleotides were synthesized by Eurofins MWG Operon (Ebersberg, Germany). The following antibodies were used: monoclonal anti-ABCG2 antibody (BXP-53) (Santa Cruz Biotechnology), monoclonal anti- $\beta$ -actin antibody (Sigma–Aldrich), alkaline phosphatase (AP)-conjugated antibodies goat anti-rat IgG (Santa Cruz Biotechnology) and AP-goat anti-mouse IgG (Promega, Mannheim, Germany).

### 2.2. Cell culture

Madin–Darby canine kidney II cells stably transfected with human ABCG2 (MDCKII-hABCG2) were kindly provided by Dr. Alfred Schinkel (The Netherlands Cancer Institute, Amsterdam, the Netherlands) and maintained as previously described [12].

### 2.3. Synthesis and cloning of cDNA

Total RNA was prepared from frozen placenta tissue of two Chinchilla rabbits obtained on gestational day 28 by caesarean section using the RNeasy Mini system (Qiagen, Hilden, Germany). Reverse transcription into cDNA was performed with Omniscript

RT-Kit (Qiagen). The rbABCG2 cDNAs were amplified using 10 pmol of the primer combinations shown in Table 1 and the Advantage2PCR Kit (Clontech, Heidelberg, Germany) with 40 cycles of 30 s at 95 °C, 30 s at 60 °C and 3 min at 68 °C. PCR products were either cloned directly into pCR XL-TOPO using the TOPO XL PCR Cloning Kit (Invitrogen) or following isolation from the agarose gel (SeaKern GTG Agarose, Lonza, Basel, Switzerland) with the QIAquick GelExtraction kit (Qiagen) into pCR4-TOPO using the TOPO TA Cloning Kit (Invitrogen, Thermo Fisher Scientific, Waltham, MA). Chemically competent *Escherichia coli* TOP10 (Invitrogen) were transformed with the ligation products and plasmid DNA was isolated from overnight cultures of kanamycin (50  $\mu$ g/ml) resistant clones using the QIAprep Spin Miniprep kit (Qiagen). Positive plasmid DNA containing the amplified fragments was assessed by agarose gel electrophoresis following treatment with EcoRI and by sequencing (performed by Qiagen or SeqLab, Göttingen, Germany). One clone representing the consensus sequence was subcloned into the mammalian expression vector pIRESneo3 (Clontech) and the resulting nucleotide sequence of prbABCG2-IRESneo3 was confirmed by sequencing.

### 2.4. Sequence analysis

Obtained sequences were analyzed using Applied Biosystems Sequence Scanner v1.0. Primer design, sequence assembly and multiple and pairwise alignment was carried out based on the ClustalW algorithm or the Jotun Hein method, respectively, using DNASTar (DNASTAR Inc., Madison, WI). Sequence homology searches were performed using the BLAST algorithm on the genetic sequence database at the National Center for Biotechnology Information (NCBI, Bethesda, MD). Protein topology predictions were performed with TM-Pred ([www.ch.embnet.org](http://www.ch.embnet.org)), PSORTII (<http://psort.hgc.jp/>), OCTOPUS ([octopus.cbr.su.se](http://octopus.cbr.su.se)) and the Split 4.0 Membrane Protein Secondary Structure Prediction Server (<http://split4.pmfst.hr/split/4/>).

### 2.5. Generation of MDCKII cells stably expressing rbABCG2

MDCKII cells were transfected with 2  $\mu$ g of prbABCG2-IRESneo3 using Effectene Transfection Kit (Qiagen) according to the manufacturer's instructions. Resistant clones were selected with 1200  $\mu$ g/ $\mu$ l G418 (Sigma–Aldrich) for 21 d and analyzed for ABCG2 expression as previously delineated [12]. Total RNA was prepared from  $3 \times 10^6$  MDCKII-rbABCG2 cells and cDNA was synthesized as recently described [13]. PCR was carried out with 1  $\mu$ l cDNA, Dream Taq PCR-Mastermix (Thermo Scientific, Waltham, MA) and 10 pmol of primers (sense: 5'-ATCAGCTCCGTTGGATCATCAGG CG-3', antisense: 5'-AAGCGTGGCCACGGACACTACTC-3'). PCR was performed over 30 cycles of 30 s at 95 °C, 30 s at 66 °C and 45 s at 72 °C.

### 2.6. Pre-treatment of MDCKII-rbABCG2, MDCKII-hABCG2 or MDCKII-WT cells

Cells were seeded in 96-well culture plates ( $8 \times 10^3$ ) and incubated for 4 h with NF (8; 80  $\mu$ M), MTX (5; 50  $\mu$ M), cimetidine (12; 120  $\mu$ M), DFM (3; 30  $\mu$ M) or with established PhIP concentrations (4; 40  $\mu$ M, [6]). Selected drug concentrations reflected the maximum human therapeutic plasma concentration ( $c_{max}$ ) and the 10-fold  $c_{max}$  serum levels [14,15]. Vehicle concentrations were generally  $\leq 0.1\%$ .

### 2.7. Cell proliferation assay

Cytotoxicity was evaluated using the WST-1 (4-[3-(4-iodophenyl)-2-(4-nitrophenyl)-2H-5-tetrazolio]-1,3-benzene

**Table 1**  
Primer pairs successfully used for amplification of rbABCG2 cDNA sequences.

No.	Oligonucleotide sequences, forward/reverse primer	product length (bp)
3	TTCTCCACAGAAAGGCAGAAAC/GCTCCTTTTAATATTAGGACAACCTAA	2047
4	AACTTACAGTTGTTTTCTCCACAGA/ACAACTCAAGGTAATTAAGGGGAATT	2043
6	CCCCACAGAAAGGCAGAAA/TAGGACAACCTCAAGGTAAT	2030

disulfonate) assay (Roche Applied Science, Mannheim, Germany) as delineated previously [16]. IC<sub>50</sub> values were defined as the substance concentration reducing the absorbance by 50% and were determined by non-linear regression analysis using Prism 5.04 (GraphPad Software Inc., San Diego, CA).

### 2.8. Hoechst H33342 accumulation assays

MDCKII-rbABCG2, MDCKII-hABCG2 or MDCKII-WT cells were seeded into 96-well cell culture plates ( $8 \times 10^3$ ). Cells were incubated with H33342 (10  $\mu$ M) for 5, 20 or 40 min in the presence or absence of Ko143 (5  $\mu$ M) or verapamil (50  $\mu$ M). To identify potential rbABCG2 interacting xenobiotics, cells were pre-treated with selected substances as described in Section 2.6. Then, H33342 (10  $\mu$ M) accumulation was determined for 40 min in the presence or absence of the test substances. Cell protein was measured using the bicinchoninic acid (BCA) assay (Pierce, Thermo Fisher Scientific, Waltham, MA). Generally, the intracellular H33342 accumulation was reported as relative fluorescence units (RFU) per mg protein in relation to untreated controls. The specific efflux activity of rbABCG2 or hABCG2 was defined as the ratio of H33342 levels in MDCKII-rbABCG2 or MDCKII-hABCG2 cells compared to that in MDCKII-WT cells.

### 2.9. SDS-PAGE and Western blot analysis

Expression of ABCG2 in MDCKII-rbABCG2 or MDCKII-WT cells was determined as previously described [12] with slight modifications. In brief, nitrocellulose membranes were probed with primary ABCG2 MAb BXP-53 (1:100) or anti- $\beta$ -actin MAb (1:7500) followed by AP-conjugated goat anti-rat IgG for ABCG2 (1:5000) or AP-conjugated goat anti-mouse IgG (1:7000) for  $\beta$ -actin.

### 2.10. Statistics

Data was analyzed with Microsoft Excel software (Office 2010). Outliers in respective test series were eliminated with a G-test. Differences between mean values of H33342 accumulation in MDCKII-rbABCG2 or MDCKII-hABCG2 cells were evaluated by one-way ANOVA followed by Fisher LSD post hoc testing using Sigma-Plot 10 (Systat Software Inc.). Differences between mean values of all other experimental test series were assessed by two-way ANOVA and the Fisher LSD post hoc test. A *p*-value of <0.05 was considered as statistically significant.

## 3. Results

### 3.1. cDNA cloning and sequencing

A consensus sequence of 2043 nucleotides (nt) was constructed from four cDNA clones obtained from two different placentas. In all eight cases, deviations from the consensus were limited to one of the four clones, allowing for an unequivocal analysis. An open reading frame of 1971 nt was identified within the sequence (Supplementary Figure 1A).

### 3.2. Predicted peptide structure of rbABCG2

Translation of the coding sequence predicts a polypeptide consisting of 656 amino acids (aa) and a molecular weight of 73 kDa (Supplementary Figure 1B). We compared this sequence with known or predicted ABCG2 protein sequences from other species including humans and other primates, laboratory and farm animals as well as *Xenopus laevis*. Sequence identity was highest (86.1 – 86.5%) with the ABCG2 peptide sequence from man, pongo and rhesus monkey, followed by mouse with 85.3% and other laboratory and farm animals with 84 – 84.4% (Table 2). *Xenopus laevis* ABCG2 exhibited a substantial lower sequence similarity (68.0%).

The rbABCG2 was predicted to contain six transmembrane domains (TMDs) with both an intracellular N-terminus and C-terminus. The localization of the TMDs was assigned to the following regions of the aa sequence: 394–417, 428–452, 467–501, 505–531, 534–559 and 627–652 (Fig. 1). In the rbABCG2 peptide sequence we further localized structural motifs known to be essential for functional ABCG2 efflux activity. These Walker A, B and C motifs were found at aa 80–87, 206–211 and 186–190 in rbABCG2, respectively (Fig. 1). The Walker A and B motifs were identical to those in human, mouse and rat with the sequences GPTGGGKS and ILFEDE. Similar to human, the sequence of the Walker C motif in rabbits was VSGGE. In rat and mouse the Walker C motif is ISGGE.

### 3.3. Generation of MDCKII cells stably expressing rbABCG2

In order to characterize rabbit placental ABCG2 transport activity, the *abcg2* gene cloned from placenta tissues of chinchilla rabbits was stably transfected in the MDCKII cell line. MDCKII-rbABCG2 clones were selected according to their transport activity (not shown) and ABCG2 expression. ABCG2 mRNA was detected in MDCKII-rbABCG2 cells while no significant transporter mRNA levels were found in the parental MDCKII cell line (MDCKII-WT) (Fig. 2A). In addition, Western blotting showed a pronounced band for the ABCG2 protein migrating at a molecular weight of around 80 kDa in rbABCG2-expressing MDCKII cells (Fig. 2B). In contrast, ABCG2 protein was not expressed in MDCKII-WT cells. Expression of  $\beta$ -actin usually served as a loading control (Fig. 2).

### 3.4. Detection of functional rbABCG2 efflux activity

Functional rbABCG2 activity was investigated with the Hoechst H33342 assay [17]. To determine the involvement of ABCG2 in cellular H33342 dye extrusion, substrate accumulation was initially measured in the presence or absence of the specific ABCG2 inhibitor Ko143 [18]. As illustrated in Fig. 3, intracellular H33342 levels were significantly reduced by around two thirds in MDCKII-rbABCG2 compared to MDCKII-WT cells. In MDCK-rbABCG2 cells, Ko143 caused a significant increase in H33342 levels by on average threefold indicating inhibition of rbABCG2-mediated H33342 cellular excretion (Fig. 3). In MDCKII-WT cells, Ko143 caused no significant alteration in H33342 levels (Fig. 3).

**Table 2**

Amino acid sequence for ABCG2 from rabbit, humans, other primates, laboratory and farm animals. Recent sequence information for rabbit was from this study or from NCBI Genbank entries for all other species (Genbank reference numbers are provided in brackets). Alignment was performed using the DNASTar software and the Clustal W algorithm. Results are expressed as percentage identity.

	1	2	3	4	5	6	7	8	9	10	
1	–										<b>rabbit</b>
2	86.4	–									<b>human</b> (NM_004827.2)
3	86.1	98.1	–								<b>pongo</b> (XM_002814957.2)
4	86.5	96.8	97.1	–							<b>rhesus monkey</b> (NM_001032919.1)
5	85.3	82.1	81.7	82.7	–						<b>mouse</b> (NM_011920.3)
6	84.4	81.5	81.6	82.2	92.8	–					<b>Rat</b> (NM_181381.2)
7	84.1	82.9	82.9	83.5	81.5	80.6	–				<b>dog</b> (NM_001048021.1)
8	84.3	84.6	84.1	84.4	80.1	79.7	86.5	–			<b>cattle</b> (NM_001037478.3)
9	84.1	85.6	85.4	85.5	80.6	80.1	86.9	96.7	–		<b>goat</b> (NM_001285707.1)
10	84.0	85.6	85.4	85.5	80.3	79.8	86.7	96.4	99.4	–	<b>sheep</b> (NM_001078657.1)
11	68.0	68.1	67.7	68.7	66.6	66.4	64.3	65.2	66.0	66.2	<b>Xenopus laevis</b> (NM_001097672.1)

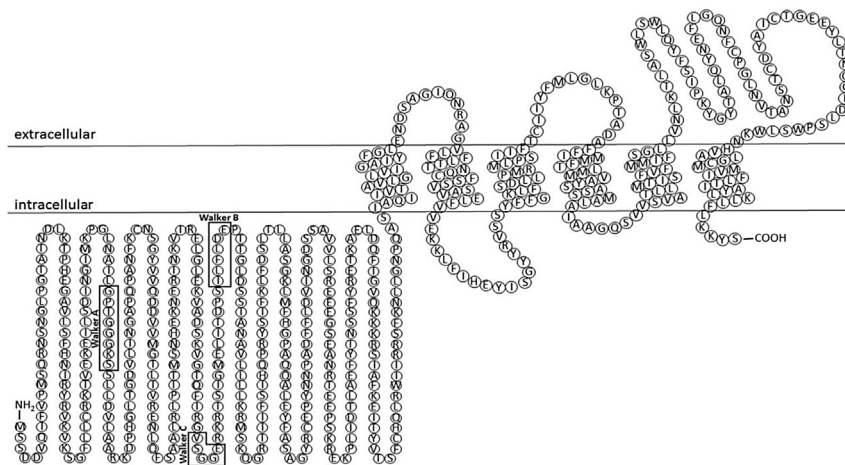


**Fig. 1.** Prediction of the rbABCG2 peptide structure and important structural motifs. Identification of the open reading frame from the consensus cDNA sequence of ABCG2 from rabbit placenta, translation and localization of Walker motifs was performed using the DNASTar software package. The two-dimensional topology of the resulting polypeptide was predicted using TM-Pred, PSORTII, OCTOPUS and Split 4.0.

### 3.5. Impact of Ko143 and verapamil on H33342 accumulation in rbABCG2 or hABCG2-transduced MDCKII cells

To compare functional efflux activity of rbABCG2 with the human ABCG2 (hABCG2) transporter, we measured the time-dependent H33342 accumulation in MDCKII-rbABCG2 and MDCKII-hABCG2 cells. In both cell lines, we observed an initial uptake phase of H33342 within the first 20 min followed by a plateau phase with steady state substrate levels. Incubation with the ABCG2 inhibitor Ko143 resulted in a significant increase in cellular H33342 levels by approximately 3.5-fold in MDCK-rbABCG2 (Fig. 4A) and around tenfold in MDCKII-hABCG2 cells (Fig. 4B) after 40 min. In both cell lines, the P-glycoprotein (P-gp) inhibitor verapamil caused no substantial alteration in the H33342 accumulation (Fig. 4).

### 3.6. Effect of hABCG2 substrates on H33342 accumulation in MDCKII-rbABCG2 or MDCKII-hABCG2 cells

In order to compare the substrate specificity of the rbABCG2 clone with hABCG2, we examined the effect of the established hABCG2 substrates PhIP [6], NF [5], DFM [19], MTX [4] and cimetidine [20] on ABCG2-mediated H33342 efflux in MDCKII-rbABCG2 or MDCKII-hABCG2 cells. Potential substrates will interact with the ABCG2 transporter and therefore can be identified in the Hoechst assay through their inhibition of cellular H33342 excretion

[17]. This inhibitory effect manifests in elevated intracellular H33342 levels in MDCKII-rbABCG2 or MDCKII-hABCG2 compared to untreated control cells. Besides, unspecific substrate accumulation was taken into account in all experiments through normalization to the corresponding H33342 accumulation in MDCKII-WT cells.

Before initiation of transport experiments, we determined short-term cytotoxicity (4 h) of the test substances in MDCKII cultures by the WST-1 assay. An  $IC_{50}$ -value of  $\sim 918 \mu\text{M}$  was obtained for NF. The highest NF concentration without a measurable effect on cell viability was  $400 \mu\text{M}$  (not shown). Cell viability remained  $>50\%$  after incubation with the highest applied concentration of PhIP ( $400 \mu\text{M}$ ), DFM ( $300 \mu\text{M}$ ), MTX ( $500 \mu\text{M}$ ) or cimetidine ( $2400 \mu\text{M}$ ) (not shown). Hence, we could not obtain an  $IC_{50}$ -value for these substances.

As shown in Fig. 5A, the hABCG2 model substrate PhIP caused a dose-dependent significant inhibition of H33342 excretion in rbABCG2 and hABCG2 clones, which was more pronounced at  $40 \mu\text{M}$  PhIP in hABCG2-compared to rbABCG2-expressing MDCKII cells. One- and tenfold NF plasma concentrations significantly blocked rbABCG2 as well as hABCG2-mediated cellular H33342 efflux (Fig. 5B). After incubation with NF serum levels, intracellular H33342 levels corresponded to almost two-times (MDCKII-rbABCG2) and about 2.5-fold (MDCKII-hABCG2) the untreated control level (Fig. 5B). The fluoroquinolone antibiotic DFM caused a significant dose-dependent inhibition of ABCG2-mediated H33342

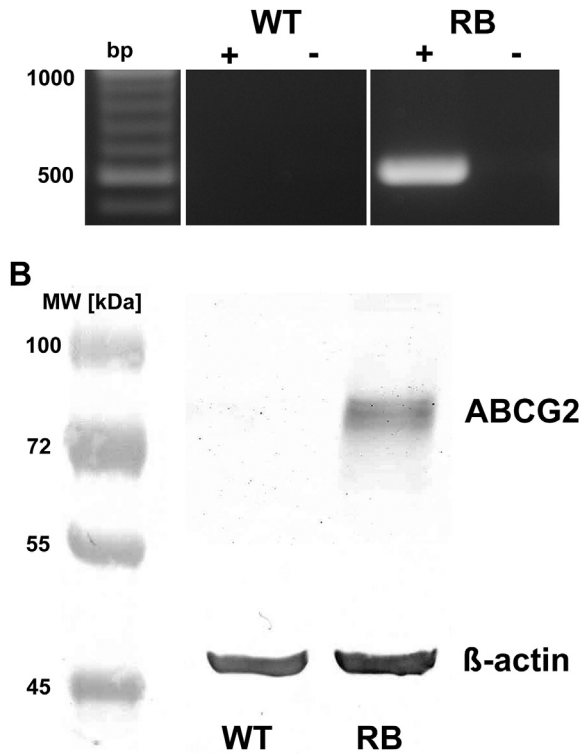


**Fig. 2.** Expression of rbABCG2 in MDCKII cells. (A) Total RNA isolated from  $3 \times 10^6$  cells was used for RT-PCR analysis of rbABCG2-transduced or MDCKII-WT cells as described in the Material and Methods Section 2.7. (B) Western blot analysis of the MDCKII-rbABCG2 and MDCKII-WT cell line was performed with 30  $\mu$ g of total protein separated on a 7.5% polyacrylamide gel. ABCG2 was detected using monoclonal antibody BXP-53 and is apparent at ~72–80 kDa ( $\rightarrow$ ).  $\beta$ -actin was used as a loading control and is apparent at ~45 kDa ( $\rightarrow$ ). The results shown are representative of two independent experiments.

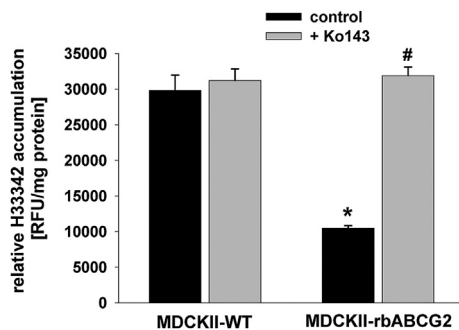


**Fig. 3.** Functional efflux activity of rabbit placental ABCG2. MDCKII-rbABCG2 or -WT cells were incubated with 10  $\mu$ M Hoechst H33342 in presence or absence of the specific ABCG2 inhibitor Ko143 (5  $\mu$ M) for 20 min. Efflux activity of rbABCG2 was measured fluorometrically as the time-dependent reduction of intracellular H33342 accumulation as delineated in the Material and Methods section. MDCKII-WT cells lacking ABCG2 expression served as a control. Finally, H33342 accumulation was expressed as RFU per mg protein. The results represent the mean  $\pm$  SEM (\* $p$  < 0.001 significance to MDCKII-WT control cells, # $p$  < 0.001 to untreated MDCKII-rbABCG2 cells, two-way ANOVA, Fisher LSD post hoc test,  $n$  = 6).

excretion in both cell lines (Fig. 5C). Compared to the untreated control, DFM plasma concentrations blocked the H33342 efflux resulting in ~1.7-fold elevated substrate levels in MDCKII-rbABCG2 cells and by on average 1.5-fold in the hABCG2 clone. As illustrated in Fig. 5D, MTX significantly inhibited the H33342 efflux in both ABCG2 clones with a dose-dependent effect only observed with rbABCG2. In relation to untreated control cells, treatment with one-

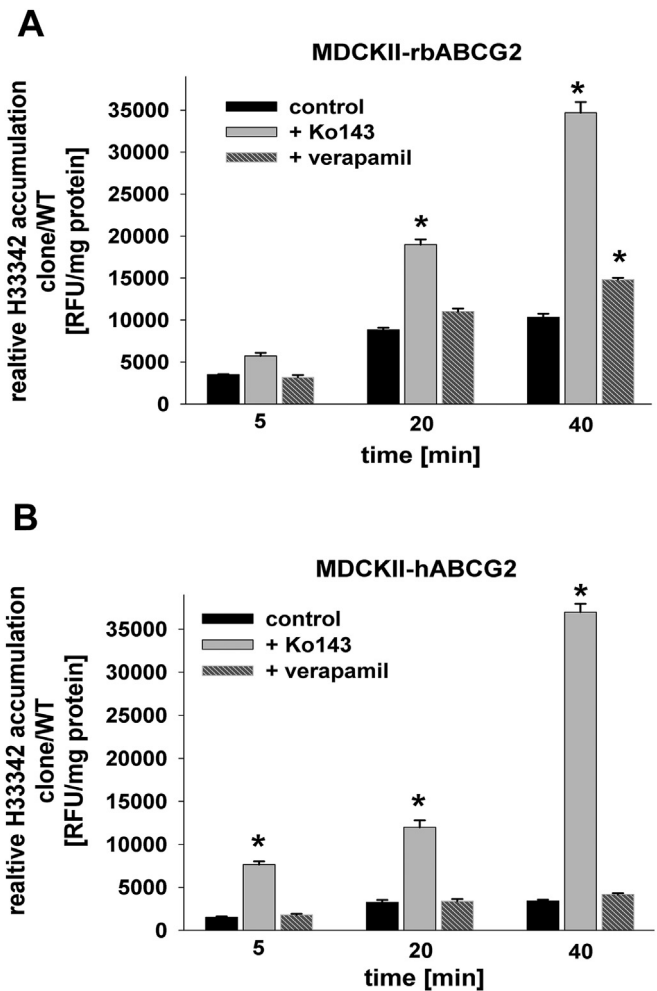


**Fig. 4.** Impact of Ko143 and verapamil on cellular Hoechst H33342 excretion in MDCKII-rbABCG2 or -hABCG2 cells. Cells were incubated with H33342 (10  $\mu$ M) for 5, 20 or 40 min in the presence or absence of the ABCG2 inhibitor Ko143 or the P-gp inhibitor verapamil as delineated in the Material and Methods Section 2.8. ABCG2 efflux activity was determined as described in the legend of Fig. 3. Values are mean  $\pm$  SEM (\*\* $p$  < 0.01, \*\*\* $p$  < 0.001 significance to untreated control cells, one-way ANOVA, Fisher LSD post hoc test,  $n$  = 12).

fold MTX serum levels resulted in a ~1.6-fold and ~2.2-fold increase in H33342 levels in MDCKII-rbABCG2 and -hABCG2 cells, respectively (Fig. 5D). Both concentrations of cimetidine significantly blocked H33342 efflux in rbABCG2-expressing cells resulting in a 1.5-fold increase of H33342 control levels (Fig. 5E). In the MDCKII-hABCG2 cell line, we observed a dose-dependent inhibition of H33342 excretion manifesting in a doubling of cellular H33342 levels with cimetidine plasma concentrations. Generally, only NF plasma concentrations caused a significant stronger inhibition of H33342 efflux in the hABCG2 compared to the rbABCG2 clone (Fig. 5B). Serum levels of all other tested drugs or 4  $\mu$ M PhIP had a similar inhibitory effect on cellular H33342 excretion in both ABCG2 clones (Fig. 5).

#### 4. Discussion

In humans, the ABCG2 efflux transporter substantially contributes to the fetoprotective placental barrier function. Due to the similar morphology of the human and the rabbit placenta [8], developmental toxicity studies of chemicals are preferably performed in rabbit [7].

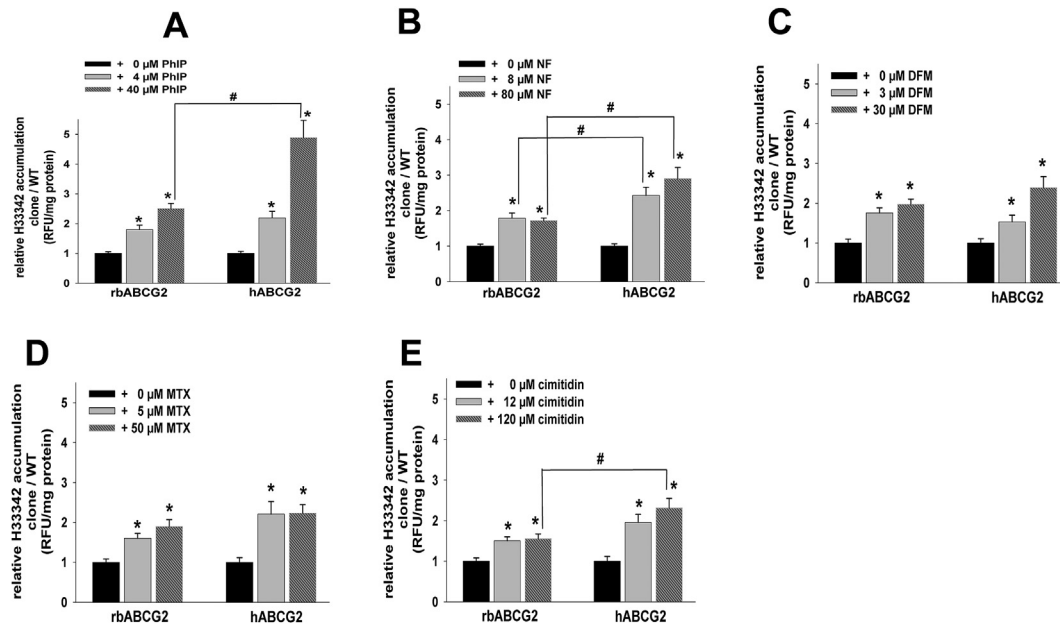


**Fig. 5.** Impact of PhIP and selected drugs on Hoechst H33342 accumulation in MDCKII-rbABCG2 or hABCG2 cells. ABCG2 clones were pre-treated (4 h) with one- and tenfold therapeutic plasma concentrations of selected drugs or the toxin PhIP. Subsequently, cells were incubated for 40 min with H33342 (10  $\mu$ M) in presence or absence of PhIP (A), NF (B), DFM (C), MTX (D) or cimetidine (E). ABCG2 efflux activity was assessed as delineated in the legend of Fig. 3. Data represent the mean  $\pm$  SEM (\* $p$  < 0.05 significance to untreated control cells, # $p$  < 0.05 significance to MDCKII-hABCG2 cells, two-way ANOVA, Fisher LSD post hoc test,  $n$  = 12).

As there is no data so far available on functional rabbit ABCG2 expression, we cloned the ABCG2 transporter from chinchilla rabbit placenta tissues. The cDNA clone was referred to as rbABCG2 henceforward. The first hypothetical rabbit ABCG2 mRNA sequence was predicted in 2010 at the time of the initiation of our study (GenBank accession no. XM\_002716965). Pairwise alignment of rbABCG2 with this hypothetical ABCG2 mRNA sequence shows good agreement in the terminal regions. However, compared to the rbABCG2, the nt 1416 to 1534 of the cDNA sequence were replaced in the predicted mRNA by an unrelated stretch of 96 nt. Consequently, on the polypeptide level, this would relate to a loss of the amino acids (aa) 458 to 498 and probably result in a non-functional transport protein. Recently, a new automated computational rabbit ABCG2 mRNA sequence prediction became available (Genbank accession no. XM\_008267616). Here, pairwise alignment with rbABCG2 showed a high degree of identity in the overlapping cDNA/mRNA sequence, amounting to 99.6% within the predicted ORF. Moreover, the aa sequences were identical when predicted from the consensus rbABCG2 cDNA and this hypothetical mRNA. Interestingly, Western blot analysis of the rbABCG2 clone produced bands slightly higher as the predicted molecular weight of rbABCG2 (Mr 72,912). This is in line with previous data of ruminant ABCG2 [12] and probably corresponds to the core- and fully glycosylated carrier protein as shown previously for human ABCG2 [21]. However, previous studies indicate that the ABCG2 glycosylation status neither significantly effects cellular expression, protein half-life, the trafficking to the plasma membrane nor the overall functional efflux activity of the ABCG2 transporter [22].

In order to examine the functional transport activity of rbABCG2 we aimed to establish a suitable cell culture model of the rabbit placental barrier. The blood-placental barrier is generally composed of tight-junctioned syncytiotrophoblasts with an apical side facing the maternal blood and a basolateral side facing the fetal fenestrated capillaries [23]. Normally, human primary cytotrophoblasts or human choriocarcinoma BeWo, JEG-3 or JAR cells are used as in vitro placenta models. However, none of these cells are

suggested as sufficiently standardized placenta barrier models [4,24]. Therefore, we stably transduced the rbABCG2 clone in MDCKII cells. The MDCKII cell line represents a well-established in vitro tool for the study of ABCG2-mediated substrate transport [17,25]. Similarly to the placenta barrier in vivo, MDCKII cells derived from kidney tubule epithelia form polarized monolayers with functional tight junctions [26]. Moreover, MDCK cells and placenta tissues show a similar expression pattern of ABC multi-drug transporters like ABCG2 [24]. Therefore, MDCKII-rbABCG2 cells overall represent an adequate in vitro tool to study ABCG2-mediated transport of xenobiotics in rabbit placenta.

Using the H33342 accumulation assay and the specific ABCG2 inhibitor Ko143, we demonstrated functional efflux activity of the ABCG2 transporter from rabbit placenta. Similarly, the specific ABCG2-mediated transport of H33342 was shown in rabbit corneal limbus epithelial cells [10]. The Hoechst dye is also a substrate of the ABC efflux transporter P-glycoprotein (P-gp) [27]. However, the P-gp inhibitor verapamil did not block the initial (20 min) H33342 efflux and had only a slight inhibitory effect on H33342 accumulation in MDCKII-rbABCG2 cells for 40 min. Hence, H33342 efflux can be clearly attributed to functional rbABCG2 activity. The detection of functional rbABCG2 activity is corroborated by the identification of important structural features in the predicted rbABCG2 protein including six TMDs. This is similar to all ABCG subfamily members that are present as half-transporters [28]. Moreover, we identified Walker A and B motifs within the rbABCG2 peptide sequence. These motifs are highly conserved in ATP-binding proteins and are known to be vitally required for ABC carrier-mediated transport [28].

Due to interspecies differences, data derived in animal studies are difficult to translate directly to human. Hence, we investigated rbABCG2 substrate specificity compared to that of the human ABCG2 (hABCG2) transporter. Therefore, we investigated interactions between selected hABCG2 substrates with rbABCG2 in comparison to hABCG2. Using the established H33342 screening assay [12,17], we identified the food carcinogen PhIP as a potential

substrate of the ABCG2 efflux transporter in rabbit placenta. Concordantly, ABCG2 was shown to decrease the PhIP fetal–maternal concentration ratio in perfused human placenta [6]. Additionally, we detected rbABCG2–drug interactions with therapeutic plasma concentrations of all tested drugs. Hence, our data suggest that the drugs NF, MTX, cimetidine, and DFM are rbABCG2 substrates. Concordantly, studies in *Abcg2*<sup>−/−</sup> mice and rat perfused placenta showed that *Abcg2* significantly limits fetal exposure with NF and cimetidine, respectively [29,30]. Moreover, the observed blockage of H33342 excretion by the tested compounds was comparable in rbABCG2- and hABCG2-expressing MDCKII-cells. Hence, our study altogether suggests a similar drug interaction potential of the rabbit and human ABCG2 transporter. This assumption is corroborated by the high peptide sequence identity of rbABCG2 and hABCG2. Interestingly, no other of the examined mammals showed a higher sequence similarity to the primates than the rabbit. However, the Hoechst assay represents an indirect setup and therefore does not clearly distinguish between ABCG2 substrates and inhibitors [17]. Our results will therefore be validated by further transepithelial transport studies [25]. Additionally, MDCKII cells overexpressing the ABCG2 transporter do not allow adequate kinetic analyses. Hence, the Hoechst assay in conjunction with ABCG2-transduced MDCKII cells overall allow the qualitative but not the quantitative comparison of human versus rabbit ABCG2/xenobiotic interactions. Moreover, the expression of rabbit or human ABCG2 in MDCKII cells may not reflect the transporter expression in human or rabbit placenta *in vivo*. To the best of our knowledge, there is no information so far on ABCG2 expression per gram of human or rabbit placenta tissues. Further studies using placenta tissue slices or primary placenta cells have to be performed to considerate species-specific difference in ABCG2 expression levels and the evaluation of the actual level of efflux in human compared to rabbit placenta.

Altogether, we first cloned and showed functional expression of the ABCG2 efflux transporter in rabbit placenta with a comparable drug interaction potential compared to human ABCG2. This includes drugs like NF routinely used to treat urinary tract infections in pregnancy [31] or MTX that is commonly employed in gestational trophoblastic neoplasia chemotherapy [32]. Hence, our results regarding active transport of xenobiotics in the placenta by rabbit or human ABCG2 contribute to corroborate the usefulness of the rabbit as an adequate reproductive model for testing the developmental toxicity of chemicals in human. Therefore, the MDCKII-rbABCG2 cell line may serve as a valuable *in vitro* tool for mechanistic studies in the context of developmental toxicity testing.

#### Conflict of interest statement

The authors declare that there are no conflicts of interest. **Disclaimer:** The views expressed in this article are those of the contributing authors and do not necessarily reflect those of their institution of employment.

#### Acknowledgments

We thank Cathleen Lakoma and Birte Scholz for skillful technical assistance and Stefanie Banneke (BfR Unit Reference Material and Certification) for providing rabbit placenta tissues. Funding was provided by the Federal Institute for Risk Assessment (BfR) (grant no. 1322-417 and 1329-427).

#### Appendix A. Supplementary data

Supplementary data related to this article can be found at <http://>

[dx.doi.org/10.1016/j.placenta.2015.12.005](http://dx.doi.org/10.1016/j.placenta.2015.12.005).

#### References

- [1] M. Iqbal, M.C. Audette, S. Petropoulos, W. Gibb, S.G. Matthews, Placental drug transporters and their role in fetal protection, *Placenta* 33 (2012) 137–142.
- [2] R. Allikmets, L.M. Schriml, A. Hutchinson, V. Romano-Spica, M. Dean, A human placenta-specific ATP-binding cassette gene (ABCP) on chromosome 4q22 that is involved in multidrug resistance, *Cancer Res.* 58 (1998) 5337–5339.
- [3] S. Lindner, S. Halwachs, L. Wassermann, W. Honscha, Expression and sub-cellular localization of efflux transporter ABCG2/BCRP in important tissue barriers of lactating dairy cows, sheep and goats, *J. Vet. Pharmacol. Ther.* 36 (2013) 562–570.
- [4] Q. Mao, BCRP/ABCG2 in the placenta: expression, function and regulation, *Pharm. Res.* 25 (2008) 1244–1255.
- [5] G. Merino, J.W. Jonker, E. Wagenaar, A.E. van Herwaarden, A.H. Schinkel, The breast cancer resistance protein (BCRP/ABCG2) affects pharmacokinetics, hepatobiliary excretion, and milk secretion of the antibiotic nitrofurantoin, *Mol. Pharmacol.* 67 (2005) 1758–1764.
- [6] P. Myllynen, M. Kumm, T. Kangas, M. Ilves, E. Immonen, J. Rysä, et al., ABCG2/BCRP decreases the transfer of a food-born chemical carcinogen, 2-amino-1-methyl-6-phenylimidazo[4,5-b]pyridine (PhIP) in perfused term human placenta, *Toxicol. Appl. Pharmacol.* 232 (2008) 210–217.
- [7] OECD, OECD Guideline for the Testing of Chemicals No. 414, Prenatal Developmental Toxicity Study, Paris, 2011.
- [8] B. Fischer, P. Chavatte-Palmer, C. Viebahn, A. Navarrete Santos, V. Duranthon, Rabbit as a reproductive model for human health, *Reproduction* 144 (2012) 1–10.
- [9] EC. European Commission Staff Working Document, accompanying document to the Seventh Report on the Statistics on the Number of Animals used for Experimental and other Scientific Purposes in the Member States of the European Union. SWD(2013)497 final. Brussels, 05/12/2013.
- [10] O.B. Selver, A. Barash, M. Ahmed, J.M. Wolosin, ABCG2-dependent dye exclusion activity and clonal potential in epithelial cells continuously growing for 1 month from limbal explants, *Invest Ophthalmol. Vis. Sci.* 52 (2011) 4330–4337.
- [11] J. Verstraelen, S. Reichl, Expression analysis of MDR1, BCRP and MRP3 transporter proteins in different *in vitro* and *ex vivo* cornea models for drug absorption studies, *Int. J. Pharm.* 441 (2013) 765–775.
- [12] L. Wassermann, S. Halwachs, S. Lindner, K.U. Honscha, W. Honscha, Determination of functional ABCG2 activity and assessment of drug-ABCG2 interactions in dairy animals using a novel MDCKII *in vitro* model, *J. Pharm. Sci.* 102 (2013) 772–784.
- [13] S. Halwachs, L. Wassermann, W. Honscha, A novel MDCKII *in vitro* model for assessing ABCG2–drug interactions and regulation of ABCG2 transport activity in the caprine mammary gland by environmental pollutants and pesticides, *Toxicol. Vitro* 28 (2014) 432–441.
- [14] F.P. Meyer, Indicative therapeutic and toxic drug concentrations in plasma: a tabulation, *Int. J. Clin. Pharmacol. Ther.* 32 (1994) 71–81.
- [15] Vetpharm: <http://www.vetpharm.uzh.ch>; last access: 09/24/2014.
- [16] S. Halwachs, C. Kneuer, W. Honscha, Downregulation of the reduced folate carrier transport activity by phenobarbital-type cytochrome P450 inducers and protein kinase C activators, *Biochim. Biophys. Acta* 1768 (2007) 1671–1679.
- [17] C. Hegedus, G. Szakács, L. Homolya, T.I. Orbán, A. Telbisz, M. Jani, et al., Ins and outs of the ABCG2 multidrug transporter: an update on *in vitro* functional assays, *Adv. Drug Deliv. Rev.* 61 (2009) 47–56.
- [18] J.D. Allen, A. van Loevezijn, J.M. Lakhai, M. van der Valk, O. van Tellingen, G. Reid, et al., Potent and specific inhibition of the breast cancer resistance protein multidrug transporter *in vitro* and in mouse intestine by a novel analogue of fumitremorgin C, *Mol. Cancer Ther.* 1 (2002) 417–425.
- [19] B. Barrera, J.A. Otero, E. Egidio, J.G. Prieto, A. Seelig, A.I. Álvarez, et al., The anthelmintic triclabendazole and its metabolites inhibit the membrane transporter ABCG2/BCRP, *Antimicrob. Agents Chemother.* 56 (2012) 3535–3543.
- [20] P. Pavek, G. Merino, E. Wagenaar, E. Bolscher, M. Novotna, J.W. Jonker, et al., Human breast cancer resistance protein: interactions with steroid drugs, hormones, the dietary carcinogen 2-amino-1-methyl-6-phenylimidazo(4,5-b)pyridine, and transport of cimetidine, *J. Pharmacol. Exp. Ther.* 312 (2005) 144–152.
- [21] K. Mohrmann, M.A. van Eijndhoven, A.H. Schinkel, J.H. Schellens, Absence of N-linked glycosylation does not affect plasma membrane localization of breast cancer resistance protein (BCRP/ABCG2), *Cancer Chemother. Pharmacol.* 56 (2005) 344–350.
- [22] N.K. Diop, C.A. Hrycyna, N-Linked glycosylation of the human ABC transporter ABCG2 on asparagine 596 is not essential for expression, transport activity, or trafficking to the plasma membrane, *Biochemistry* 44 (2005) 5420–5429.
- [23] J. Behravan, M. Piquette-Miller, Drug transport across the placenta, role of the ABC drug efflux transporters, *Expert Opin. Drug Metab. Toxicol.* 3 (2007) 819–830.
- [24] C. Prouillac, S. Lecoœur, The role of the placenta in fetal exposure to xenobiotics: importance of membrane transporters and human models for transfer studies, *Drug Metab. Dispos.* 38 (2010) 1623–1635.
- [25] L. Wassermann, S. Halwachs, D. Baumann, I. Schaefer, P. Seibel, W. Honscha,

- Assessment of ABCG2-mediated transport of xenobiotics across the blood-milk barrier of dairy animals using a new MDCKII in vitro model, *Arch. Toxicol.* 87 (2013) 1671–1682.
- [26] J.D. Irvine, L. Takahashi, K. Lockhart, J. Cheong, J.W. Tolan, H.E. Selick, et al., MDCK (Madin-Darby canine kidney) cells: A tool for membrane permeability screening, *J. Pharm. Sci.* 88 (1999) 28–33.
- [27] J.G. Sarver, W.A. Klis, J.P. Byers, P.W. Erhardt, Microplate screening of the differential effects of test agents on Hoechst 33342, rhodamine 123, and rhodamine 6G accumulation in breast cancer cells that overexpress P-glycoprotein, *J. Biomol. Screen* 7 (2002) 29–34.
- [28] P. Krishnamurthy, J.D. Schuetz, Role of ABCG2/BCRP in biology and medicine, *Annu. Rev. Pharmacol. Toxicol.* 46 (2006) 381–410.
- [29] F. Staud, Z. Vackova, K. Pospechova, P. Pavek, M. Ceckova, A. Libra, et al., Expression and transport activity of breast cancer resistance protein (Bcrp/Abcg2) in dually perfused rat placenta and HRP-1 cell line, *J. Pharmacol. Exp. Ther.* 319 (2006) 53–62.
- [30] Y. Zhang, H. Wang, J.D. Unadkat, Q. Mao, Breast cancer resistance protein 1 limits fetal distribution of nitrofurantoin in the pregnant mouse, *Drug Metab. Dispos.* 35 (2007) 2154–2158.
- [31] J. Le, G.G. Briggs, A. McKeown, G. Bustillo, Urinary tract infections during pregnancy, *Ann. Pharmacother.* 38 (2004) 1692–1701.
- [32] J.R. Lurain, Gestational trophoblastic disease II: classification and management of gestational trophoblastic neoplasia, *Am. J. Obstet. Gynecol.* 204 (2011) 11–18.